MNRAS **000**, 1–13 (2018) Preprint 16 August 2019 Compiled using MNRAS LATEX style file v3.0

Understanding the significant effect of photometry on galaxy pair fractions using the stellar-mass-halo-mass connection.

Philip J. Grylls,[1]★ F. S. Shankar,[1] C.C,[2]
[1]*Southampton*
[2]*Nottingham*

Accepted XXX. Received YYY; in original form ZZZ

ABSTRACT
This paper shows the connection between the choice of photometry in construction of the stellar mass function and the pair fraction of galaxies found using STEEL, the Statistical sEmi-Emprical modeL. It is know that pair fractions, the number of galaxies found with a massive companion, are sensitive to choices made when selecting what qualifies as a pair, for example luminosity or stellar mass selections. It has been found by using different photometries that the stellar mass function is significantly higher for massive galaxies than previously thought. We assess the systematic changes that this new stellar mass function may have on the pair fraction by compare mock clustering samples made using STEEL . The galaxy halo connection is constrained using the stellar-mass-halo-mass relationship for two observed stellar mass functions, the Illustris TNG stellar mass function, and for a suit of toy models. From each of these connections the pair fraction, and its evolution, is generated. It is found that enhancements to the number density of high mass galaxies cause the pair fraction to be smaller and that the evolution of the abundance of the high mass galaxies is critical to the evolution of the pair fraction. We argue this is a considerable cause of bias that should be accounted for when comparing pair fractions between surveys.

Key words: keyword1 – keyword2 – keyword3

1 INTRODUCTION

ΛCDM cosmology predicts the hierarchical assembly of dark matter haloes. Early over-dense regions in the distribution of dark matter grew under the influence of gravity in mass and extent into what we refer to as dark matter haloes. Larger haloes then accreted smaller haloes further building their mass. At early epochs the gas directly follows the collapse of the dark matter sinking to the bottom of the potential wells cooling and forming stars (Mo et al. 1998). Larger dark matter haloes had a stronger gravitational influence creating a deeper potential well capturing more gas and are thus associated with larger galaxies. The connection between large galaxies and large dark matter haloes results in larger galaxies experiencing many more galaxy mergers due to the denser environment. Massive galaxies are therefore able to grow by accretion of stellar mass from satellite as well as star formation.

Frequent or massive mergers are thought to be causes of morphological change in galaxies especially in more massive spheroidal systems. Galaxies after experiencing a massive merger, where the minor galaxy is at least a quarter of the mass of the central galaxy, are thought to loose their disk like morphology and be transformed into elliptical galaxies Negroponte & White (1983); De Lucia et al. (2006). For this reason it is important to understand the frequency and nature of mergers between galaxies to achieve a complete and coherent picture of galaxy formation and evolution. However, galaxy mergers occur on gigayear timescales and therefore it is not possible to directly measure the rate and corresponding consequence of galaxy mergers. The traditional approach to measure galaxy mergers is to instead count galaxy pairs, at a given separation, and then assign a merging timescale to estimate the rate of galaxy merging (Conselice et al. 2003, 2008; Mundy et al. 2017). This approach is complicated by systematic discrepancies arising from galaxy pair measurements that selecting galaxies by flux or stellar mass (Man et al. 2016).

In Grylls et al. (2019) (Hereafter Paper I) we introduce we introduce a the Statistical sEmi-Empirical modeL, STEEL. STEEL and other transparent semi-empirical approaches have had multiple successes:

★ E-mail: mn@ras.org.uk (KTS)

- Mapping galaxies into dark matter haloes using the stellar-mass-halo-mass relation, derived from the relative abundance of dark matter haloes and galaxies.
- Following the mergers of the underlying host dark matter halos.
- Computing the implied rate of galaxy mergers.

Amongst these outcomes the ability to predict the galaxy merger rate is particularly powerful as it provides and additional tool to test the ΛCDM cosmological model. The galaxy merger rate is intrinsically connected to the dark matter assembly so the galaxies can be used as a proxy for the dark matter structure. However, there are notable systemics that could affect the reliability of using the galaxy merger rate from models, the primary tool in this analysis is the stellar-mass-halo-mass relation which is fully dependent on the shape of the input stellar mass function. The stellar mass function is affected by several observational systematics notably, wrong choice of mass to light ratios, stellar initial mass function, light profile e.t.c... In the last decade it has been shown that the stellar mass function, the comoving number density of galaxies of a given stellar mass, is significantly higher in the high mass end than previously thought due to incomplete fitting of the extended light profile of massive galaxies(for a complete discussion see (Meert et al. 2015; Bernardi et al. 2016, 2017a)). Using Sèrsic Exponential photometry the number density of high mass galaxies is increased and this in turn steepens the high mass slope of the stellar-mass-halo-mass relationship.

The effect of the stellar mass functions and the systematics introduced into the stellar-mass halo-mass relation are investigated in Grylls et al. (2019b) (Hereafter Paper II). It is shown by estimating the total mass accreted from satellites that stellar mass functions with an enhanced high mass end, and the corresponding steeper stellar-mass-halo-mass relationships, are more consistent with ΛCDM models of hierarchical growth. Stellar mass functions with enhanced high mass number density predict galaxies grow more rapidly with cosmic time, the lower growth rates predicted by traditional stellar mass functions are lower than the satellite accretion rates and are therefore inconsistent with hierarchical assembly models. Given the pair fraction is used a an observational estimate of galaxy merger rates and satellite accretion one would expect that where stellar mass functions impact the accretion rates they should also produce an difference in modeled pair fractions.

In this work ee investigate how the observed pair fraction changes systematically with varying stellar-mass-halo-mass relationship. We use STEEL which is capable of producing state of the art galaxy clustering mocks using a statistical dark matter accretion history and the galaxy-halo connection. We show that a well designed and flexible Semi-Empirical model should be used as an essential analytic tool for understanding how observational modelling assumptions, such as the estimation of stellar mass, may propagate in unpredictable ways. This paper is laid out as follows. In Section 2 we describe the comparative simulation data used. In Section 3 we summarize STEEL the STastical sEmi-Empirical modeL from previous work and extensions added for the analysis in this work. In Section 4 we show a systematic analysis of how the stellar-mass-halo-mass relation effects the pair fraction then compare the output of STEEL using altered stellar-mass-halo-mass relations to match simulation and observational results to show the magnitude of the differences. In Sections 5 & 6 we situate our results in a wider context and conclude.

2 DATA

2.1 Illustris

We use data extracted from the Illustrius TNG simulation JupyterLab public data mirror (Springel et al. 2018; Nelson et al. 2018). Illustrius TNG is a state of the art, large volume, cosmological, gravo-magnetohydrodynamical simulation. To make comparisons to the results from STEEL we utilize the group and subhalo galaxy/dark matter catalogues to explore the distributions of galaxy pairs in group and cluster environments from Illustrius TNG.

3 METHOD

[It is critical to be able to understand how assumptions made when deriving the stellar mass function propagate further into models of galaxy formation. In Paper II we showed how different photometric choices used to derive classical stellar mass functions create central galaxy growth histories that are inconsistent with the satellite galaxy accretion predicted by hierarchical assembly. This has been missed by previous models that used hierarchical assembly models for the following reasons:

- The models may not have 'true' merger histories, Asquith et al. (2018) show how the stellar mass function predicted by many Semi-Analytic models is not correct at high redshift. As the models are tuned to match the stellar mass function at low redshift the accretion history must therefore compensate, through over or under merging, to correct the number densities.
- The models are discrete, individual galaxies are simulated rather than looking at the total population, in such 'classical' models galaxy growth and accretion are directly linked likely obscuring any issues.

Our model STEEL does not suffer from either of these effects. Firstly, it is an empirical model therefore the stellar mass function is retrieved by design at all redshifts as confirmed in Paper I, furthermore in Paper II we confirm the satellite distribution is good at all redshifts. Secondly, STEEL is designed to simulate satellite galaxies in groups and clusters without the volume or resolution limitations in 'classical' cosmological models this is achieved using a statistical dark matter accretion history, described in Section 3.3, in short we remove discrete haloes and instead look at the statistical averages for each population. The full methodology for STEEL can be found in Paper I with updates and examples of post-processing techniques found in Paper II.] In this paper we highlight difficulties present when comparing models to observations, specifically pair fractions. Foremost the difficulties stem from the assumptions inherent in a given photometric choice. For example, using the Sloan Digital Sky Survey Data Release 7 (SDSS-DR7) two notably different stellar mass functions have been derived. Using a de Vaucouleurs fit (Abazajian et al. 2009) produces a stellar mass function with

a sharp high mass cutoff, whereas, using a Sérsic + exponential model (Meert et al. 2015; Bernardi et al. 2016, 2017b) produces a less sharp cutoff and more high mass galaxies. The propagation of these differences into the stellar-mass-halo-mass relation in conjunction with hierarchical assembly predicted by ΛCDM cosmology creates different galaxy assembly histories within the same cosmology. An empirical model, such as STEEL, is ideally suited to understand these effects. By design an empirical model recreates the stellar mass functions at all redshifts, something other modeling techniques such as Semi-Analytic models have historically struggled with (Asquith et al. 2018). The reproduction of the stellar mass function at all redshifts is essential to the reproduction of correct assembly history. For example, a stellar mass function at high redshift with an excess of low mass galaxies must then self correct though over merging to match the stellar mass function at low redshift. Additionally STEEL has an advantage over other Semi-Empirical models, using a statistical dark matter accretion history to replace the discrete dark matter volumes we are able to simulate without volume or resolution constraint. In Paper I and Paper II we show that using the Sérsic + exponential fits STEEL recreates the distributions of satellite galaxies over a large range of cosmic epochs. In Paper II we showed the in-situ vs ex-situ growth ratios for central galaxies for both stellar mass functions, we found that the de Vaucoulers fit creates a satellite galaxy accretion history that is inconsistent with the predicted growth of the central galaxy. The satellite accretion/merger rate is often predicted by the the pair fraction observations, it stands to reason that the discussed discrepancies in satellite accretion should also present in the pair fraction. In this Paper we discuss the updates to STEEL that enable the extraction of pair fraction, we then show how the stellar-mass-halo-mass relation effects the expected pair fraction in a toy model. We build an understanding how we expect input stellar mass functions, and the associated photometric choice, to impact the pair fraction observation and use this to provide an explanation for discrepancies found in the observations.

In this section we begin by describing how the stellar-mass-halo-mass relation propagates into the pair fraction with the aid of two cartoons in Section 3.1, we give the quantitative fits for the stellar-mass-halo-mass relations used in this work in Section 3.2 we then describe the statistical accretion history that is the core methodology of STEEL in Section 3.3, finally we describe the update made to give a spacial distribution to the satellites in Section 3.4.

3.1 Influence of the stellar-mass-halo-mass relation

The photometric choice, or other systemics such as mass to light ratio, the initial mass function, or background subtraction, used to calculate galaxy stellar mass has a direct impact on the stellar mass function. Where the ΛCDM cosmology remains constant, i.e. the number and distribution of haloes is unchanged, changes in the stellar mass function are directly correlated to changes in the stellar-mass-halo-mass relation. The stellar-mass-halo-mass relation can therefore be used as an effective proxy for the choices made when deriving the stellar mass function as well as a tool to create create toy models to test theoretical systematic changes to the stellar mass function. [In this work we show using the two data driven (PyMorph and cModel) and a collection of 'toy' stellar-mass-halo-mass relations how different relations, and therefore different photometries, give different pair fractions and merger rates. In Figure 1 we show an illustrative cartoon of how different stellar-mass-halo-mass relations effect the galaxy mass ratios. For two halo masses we see that the slope of the stellar-mass-halo-mass relation causes a 4x difference in the stellar mass ratio mapped into the halos. In this figure the difference in slopes has been exaggerated for clarity, however, on average it is obvious that a shallower relation causes many more massive pairs than a steep relation.] In this work we show using different stellar-mass-halo-mass relations give different pair fractions and merger rates. Stellar mass functions with a greater number densities of high mass galaxies naturally map larger galaxies into larger haloes due to their relative abundances. This results in a steeper high mass slope for the stellar-mass-halo-mass relations produced by more abundant stellar mass functions. In Figure 1 we show an illustrative cartoon of how different stellar-mass-halo-mass relations effect the galaxy mass ratios. For two halo masses we see that the steeper slope of the stellar-mass-halo-mass relation causes a substantial difference in the stellar mass ratio mapped into the haloes. In general a shallower relation causes many more massive pairs than a steeper relation.

[In Figure 2 a cartoon is shown to give an example of the expected difference when changing the stellar-mass-halo-mass relation in the pair fraction, the fraction of galaxies of a given mass that have a companion with a mass equal to or greater than a quarter of the primaries mass. The left hand column shows the stellar-mass-halo-mass relations and the right the expected pair fractions with redshift, in this cartoon we show examples where the high mass slope is manipulated later in this work we show the effects of changing any parameter. In the top row we compare a steep high mass slope to a flat slope where the slope has been changed at redshift $z = 0.1$, in turn this increase the number of pairs created and the normalisation increases. In the bottom row we show the effects of having a slope that flattens with redshift to achieve this the slope evolution parameter is increased. We show the redshift $z = 0.1$ relation in grey and the relations with the unchanged and changed slope in blue and orange respectively. The effect on the pair fraction is to change the pair fraction from flat/turning over to a steadily increasing fraction with redshift. In both cases this is the behaviour one would expect given Figure 1 where shallower slopes give higher fractions. Furthermore, from this Figure and from Figure 3, shown in Section 4, almost any pair fraction shape could be produced by altering the input stellar-mass-halo-mass relation. It is also of note that whilst we focus on using two photometric choices that give a substantially different stellar-mass-halo-mass relation we find relatively minor changes can cause qualitative differences in the pair fraction.] In Figure 2 a cartoon is shown to give an example of the expected difference in the pair fraction when changing the stellar-mass-halo-mass relation. We define pair fraction as the fraction of galaxies of a given mass that have a companion with a mass equal to or greater than a quarter of the primaries mass within 5-30 kpc. The left hand column shows the stellar-mass-halo-mass relations and the right column the implied pair fractions with redshift, when varying

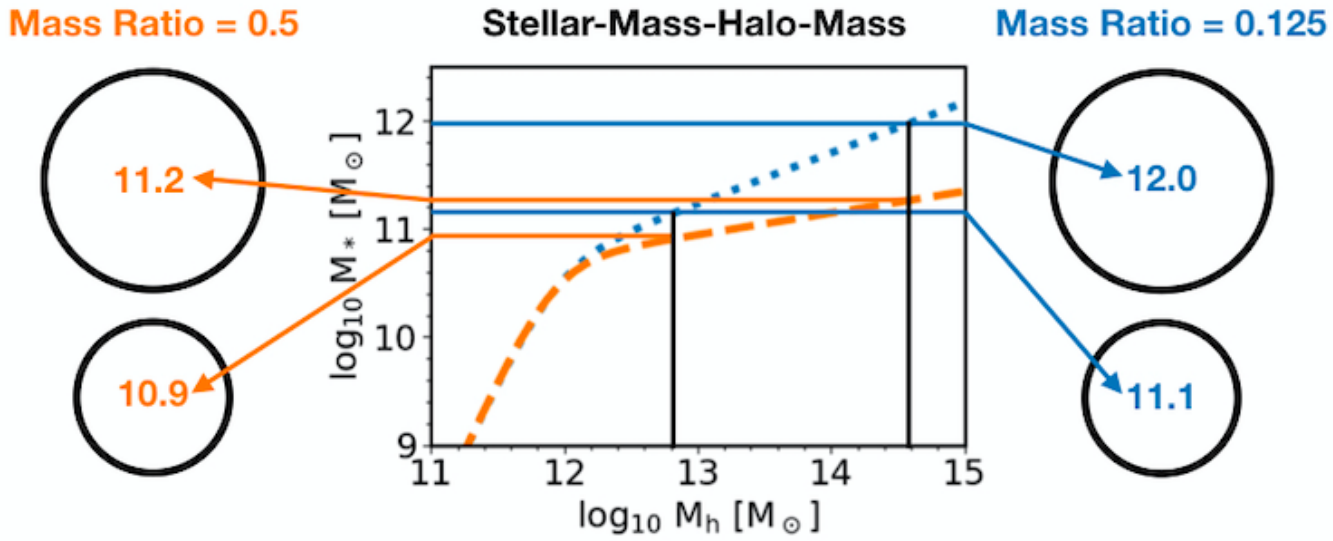

Figure 1. A cartoon showing the how the stellar-mass-halo-mass relation can impact the stellar mass ratio of galaxies mapped into identical halos. The steeper stellar-mass-halo-mass relation creates a smaller stellar mass ratio as the change in halo mass maps to a much larger stellar mass difference.

the high-mass slope of the stellar-mass-halo-mass-relation. In the top row we compare a steep high mass slope to a flat slope, where the slope has been changed at redshift $z = 0.1$. The steepening of the high mass slope increases the number of pairs created and the normalisation of the pair fraction increases. In the bottom row we show the effects of having a slope that flattens with redshift. We show the redshift $z = 0.1$ relation in grey and the relations with the unchanged and changed slopes in blue and orange respectively. The main effect of varying the slope in the stellar-mass-halo-mass relation is to change the behaviour of pair fraction with redshift. A steeper slope tends to turn over the pair fraction and vice-versa. In both cases this is the behaviour one would expect given Figure 1 where shallower slopes give higher fractions. Furthermore, from Figure 2 (and from Figure 3, shown in Section 4), it can be concluded that almost any pair fraction time dependence could be produced by appropriately altering the input stellar-mass-halo-mass relation. It is relevant to stress here relatively minor changes can cause qualitative differences in the stellar-mass-halo-mass relation and by extension in the shape and normalization of pair fractions at any cosmic epoch.

3.2 Stellar-mass-halo-mass relation

A double power-law relation similar to Moster et al. (2010) is used to parameterise the stellar-mass-halo-mass relation. The parameters M, N, β, and γ control respectively the position of the knee, the normalization, the low mass, and the high mass slope at redshift $z = 0.1$. Each parameter has an associated redshift evolution factor,

$$
\begin{aligned}
M_*(M_h, z) &= 2M_h N(z)\left[\left(\frac{M_h}{M_n(z)}\right)^{-\beta(z)} + \left(\frac{M_h}{M_n(z)}\right)^{\gamma(z)}\right]^{-1} \\
N(z) &= N_{0.1} + N_z\left(\frac{z-0.1}{z+1}\right) \\
M_n(z) &= M_{n,0.1} + M_{n,z}\left(\frac{z-0.1}{z+1}\right) \\
\beta(z) &= \beta_{0.1} + \beta_z\left(\frac{z-0.1}{z+1}\right) \\
\gamma(z) &= \gamma_{0.1} + \gamma_z\left(\frac{z-0.1}{z+1}\right).
\end{aligned}
\tag{1}
$$

We use the fits from Paper II, shown in Table 3.2, that give the parameters for a Sérsic-Exponential fit stellar mass function (PyMorph) and a de Vaucouleurs fit stellar mass function (cmodel) and for completeness, we also include a SMHM relation that well fits the outputs of the Illustris TNG.

3.3 Statistical Accretion Histories

Traditional simulations such as Hydrodynamical, Semi-Analytic or Semi-Empirical models simulate the dark matter background of the universe using a cosmological box or a discrete set of merger trees. [Each of these techniques generates a simulated 'volume', the volume of these simulations lead to small halos or low mass ratio mergers being simulated orders of magnitude more than their more massive counterparts.] Both cosmological boxes and merger trees simulate a discrete cosmological volume, in any given volume there will be a limited number of massive haloes. Due to the significant decrease in number density with increasing halo mass, haloes of even a couple of orders of magnitude smaller than the most massive halo in the simulation are found in signif-

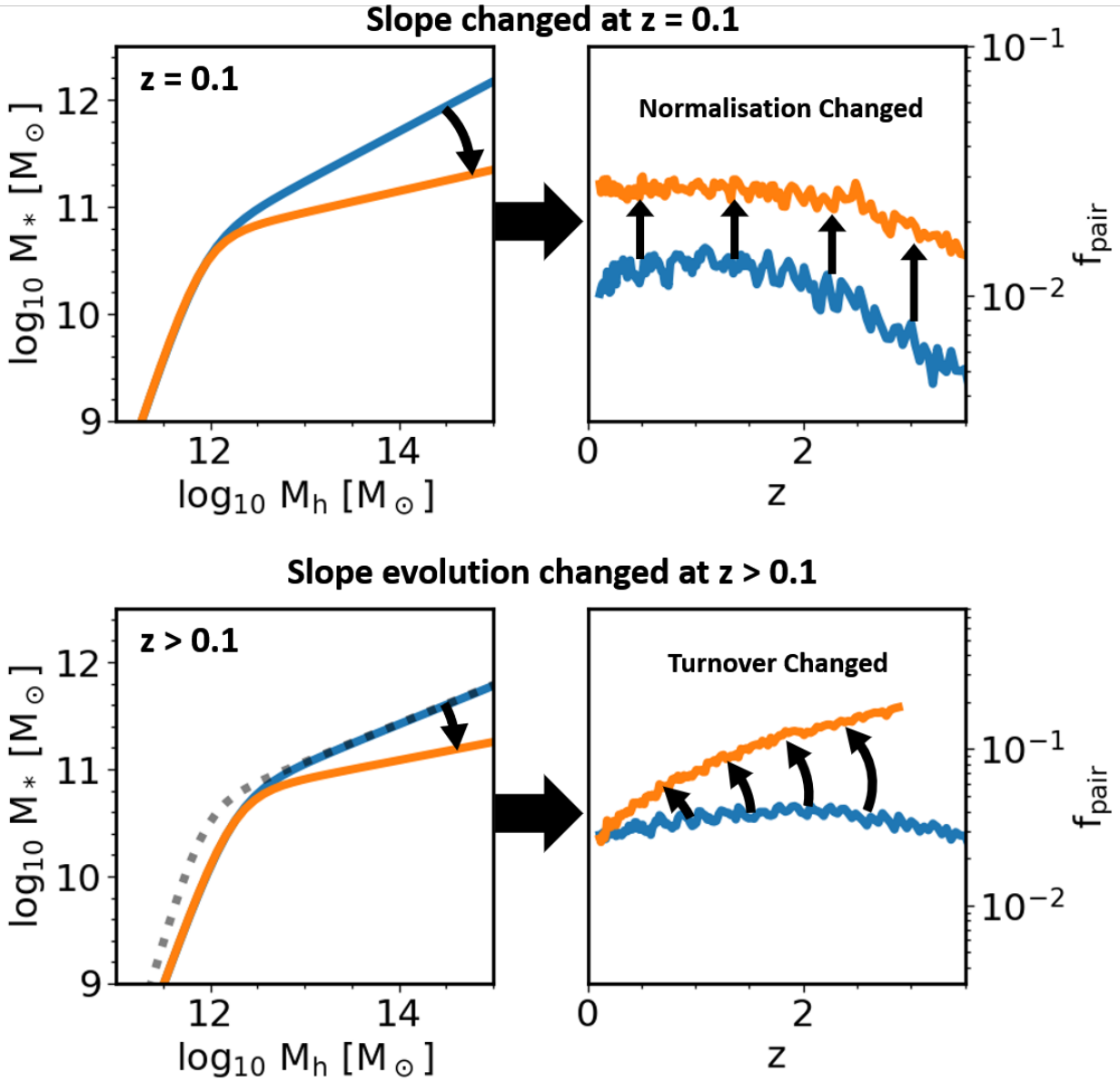

Figure 2. A cartoon showing the how the stellar-mass-halo-mass relation can impact the pair fraction. The top row shows how reducing the high mass slope of the stellar-mass-halo-mass relation increase the number of pairs at all redshifts. The bottom row shows the redshift $z = 0$ relation as a grey dotted line, two relations at redshift where the relation is not evolved or evolved to be shallower are shown in blue and orange respectively. For this evolving stellar-mass-halo-mass relation the pair fractions are found to increase. In each case the reason for the increase can be explained by referencing Figure 1 where making the relation shallower seeds more massive pairs.

	M_n	N	β	γ	$M_{n,z}$	N_z	β_z	γ_z
cmodel	$11.91^{+0.40}_{-0.34}$	$0.029^{+0.018}_{-0.013}$	$2.09^{+1.21}_{-1.02}$	$0.64^{+0.11}_{-0.10}$	$0.52^{+0.24}_{-0.19}$	$-0.018^{+0.005}_{-0.004}$	$-1.03^{+0.049}_{-0.34}$	$0.084^{+0.20}_{-0.14}$
PyMorph	$11.92^{+0.39}_{-0.36}$	$0.032^{+0.016}_{-0.012}$	$1.64^{+0.85}_{-0.73}$	$0.53^{+0.11}_{-0.11}$	$0.58^{+0.15}_{0.19}$	$-0.014^{+0.007}_{-0.006}$	$-0.69^{+0.29}_{-0.36}$	$0.03^{+0.154}_{-0.147}$
TNG	11.8	0.018	1.5	0.31	0.0	−0.01	0	−0.12

Table 1. The stellar-mass-halo-mass relation fits for cmodel, PyMorph, and TNG. For the cmodel and PyMorph data, the errors are the 16th and 86th percentile from the MCMC fiting.

icantly more frequently. Due to the discrepancy in number density mergers between haloes of simmilar mass are extremely rare especially in smaller volumes. STEEL removes the dependence on discrete halo sets by using a 'statistical accretion history': massive halos and high mass ratio mergers are simulated equally with smaller halos and low mass ratio mergers regardless of number density.

The full method for creating the 'statistical accretion history' is given in Paper I and a summary of the method is provided in Paper II. In brief, we start from the average growth history of central haloes and at each epoch compute the unevolved subhalo mass function[1]. At each time step the growth of the unevolved subhalo mass function is attributed to accretion of new subhaloes to create the accreted subhalo mass function (simply the number density of a given subhalo mass accreted at a given epoch for a given central mass history). Each bin of the accreted subhalo mass function is assigned a dynamical time, in essence the time to merge with the central galaxies. The surviving subhalo mass function[2] is created by summing each mass of accreted subhaloes at each time step that have not yet merged with their centrals by the redshift of observation. In this work we use the PyMorph abundance matching fits from Paper II to associate each bin of the accreted subhalo mass function with a distribution of galaxies at infall. The satellite galaxies associated to subhalo bins that have reached the end of their dynamical times are summed to contribute to the average galaxy accretion history for a given dark matter halo.

3.4 Galaxy Separations

Calculation of the pair fraction requires an estimation of the distance between the central galaxy and the satellite galaxy, as we rely on our statistical accretion history, and do not have discrete halos, we assign each subhalo bin an average distance to the central galaxy. The subhaloes start at the viral radius of the central halo. The distance to the centre then reduces proportionally to the amount of dynamical time remaining (Guo et al. 2011).

4 RESULTS

In this section we test the impact of two different photometry choices, PyMorph and cmodel, on the pair fractions. Fixing the dark matter halo assembly and cosmology, the two photometries generate two distinct stellar-mass-halo-mass relations where the main difference lies in the high mass slope. [Firstly, in Section 4.1 we use a toy model were the stellar-mass-halo-mass relation is manually altered from the PyMorph fit, this is done to understand how each stellar-mass-halo-mass parameter propagates into the pair fractions.] To gain deeper insight into how the input stellar-mass-halo-mass relation propagates into the pair fractions, in Section 4.1 we sequentially alter each parameter in the stellar-mass-halo-mass relation. In Section 4.2 we then attempt to recreate pair fractions found in the Illustris TNG simulation and in data. We use the toy model results to guide adjustments made to the stellar-mass-halo-mass relation to improve the match to the data. [Finally, we investigate the self consistency of the stellar-mass-halo-mass relation that best fits the observed pair fraction following the method from Paper II.] Finally, using the stellar-mass-halo-mass relation that best fits the observed pair fraction we compute satellite accretion histories, the amount of stellar mass growth expected from satellite accretion, and central stellar mass growth histories, the predicted central stellar mass growth from abundance matching. By comparing the total accreted mass and mass accretion/growth rate between the central and satellite, following the methods in Paper II, we test if the observed pair fractions create a satellite mass accretion that is consistent with the central galaxy growth.

In this Section we investigate the distribution of satellites around central galaxies when using different stellar-mass-halo-mass relations This distribution is primarily dominated by the halo substructure, for this reason it is essential to make sure our selection criteria for galaxies always returns the same halo population. As we actively change the stellar masses mapped into any given halo mass one cannot use a stellar mass cut to achieve this result. From a simulation where the haloes are known, one could simply select by halo mass, however, to better match observation where haloes are not known we make a constant number density selection. A constant number density selection will always return objects that share a given number density and are therefore associated to the same haloes as we are taking the halo structure as a fixed quantity. A simmilar technique was employed by Leja et al. (2013) to trace galaxy populations through time where galaxies at high redshift with a given comoving number density are assumed to be the progenitors of later populations with the same abundance. In this work we calculate the number density selection by, selecting a central stellar mass from PyMorph ($M_* = 10^{11} - 10^{11.6} M_\odot$ or $10^{9.5} - 10^{10.1} M_\odot$ for β), computing the number-density range of this mass cut and then selecting galaxies from the other photometries/toy models which share this number density. An example of this selection can be seen in Figure 3, the shaded horizontal band shows the stellar masses for each stellar-mass-halo-mass relation that share number density.

4.1 Systematic Analysis

We use the flexible nature of STEEL to create a toy model where each of the main parameters (M, N, β, γ), and their evolutionary factors (M_z, N_z, β_z, γ_z), governing the stellar-mass-halo-mass relation are adjusted in turn to explore the knock on systematic introduced in the galaxy pair fractions. Table 4.1 details the change made to the stellar-mass-halo-mass relation for each parameter. Figure 3 shows each of the stellar-mass-halo-mass relations in the outer four panels, the reference stellar-mass-halo-mass relation PyMorph is shown at redshifts $z = 0.1$ (dotted line) and $z = 2$ (dashed line) in each panel, the modified redshift $z = 0.1$ relation is then shown in orange, and the increased and decreased (dashed red and green) evolution are shown at redshift $z = 2$. The inner four panels follow the same colour convention.

[1] This is the total number density of subhaloes accreted by a central halo over its growth history as a function of the mass ratio M_{sat}/M_{cen} where the satellite masses are frozen at infall.
[2] The total number density of subhaloes that one would expect to still be present in the parent halo at a given epoch.

Table 2. The adjustments to the stellar-mass-halo-mass relation used in Figure 3.

	PyMorph	$X_{0.1,alt}$	$X_{z,+}$	$X_{z,-}$
M	11.92	-0.25	-	-
M_z	0.58	-	+0.1	-0.1
N	0.032	+0.04	-	-
N_z	-0.014	-	+0.007	-0.007
β	1.64	-0.3	-	-
β_z	-0.69	-	+0.3	-0.3
γ	0.53	+0.06	-	-
γ_z	-0.03	-	+0.2	-0.2

The pair fraction in the central panels is calculated as the number density of satellites with a mass ratio of above 1/4 within 5 to 30kpc of the central galaxy divided by the total number of central galaxies within the mass selection. When changing M, the knee parameter, a large increase in the pair fraction is found from a lower knee: The shallower high mass slope is extended therefore more haloes are seeded in the mass range for pairs. We see the same effect at high redshift, the lower value of M at high redshift creates a higher pair fraction. The normalization parameter, N, creates little change in the pair fraction as expected because the mass ratios are largely unaffected. The low mass slope parameter, β, affects the seeding of smaller galaxies hence a smaller mass range is used the steepness of this slope gives the difference in stellar masses used for consistency in number density to be the highest of all four parameters, it can be see at high and low redshift that steeper slopes give rise to lower pair fractions as less galaxies are seeded within the mass ratio range. Finally, when the high mass slope parameter, γ, is altered more pairs are found at high and low redshift when the slope is shallow. This is again attributed to more galaxies seeded within the mass ratio range.

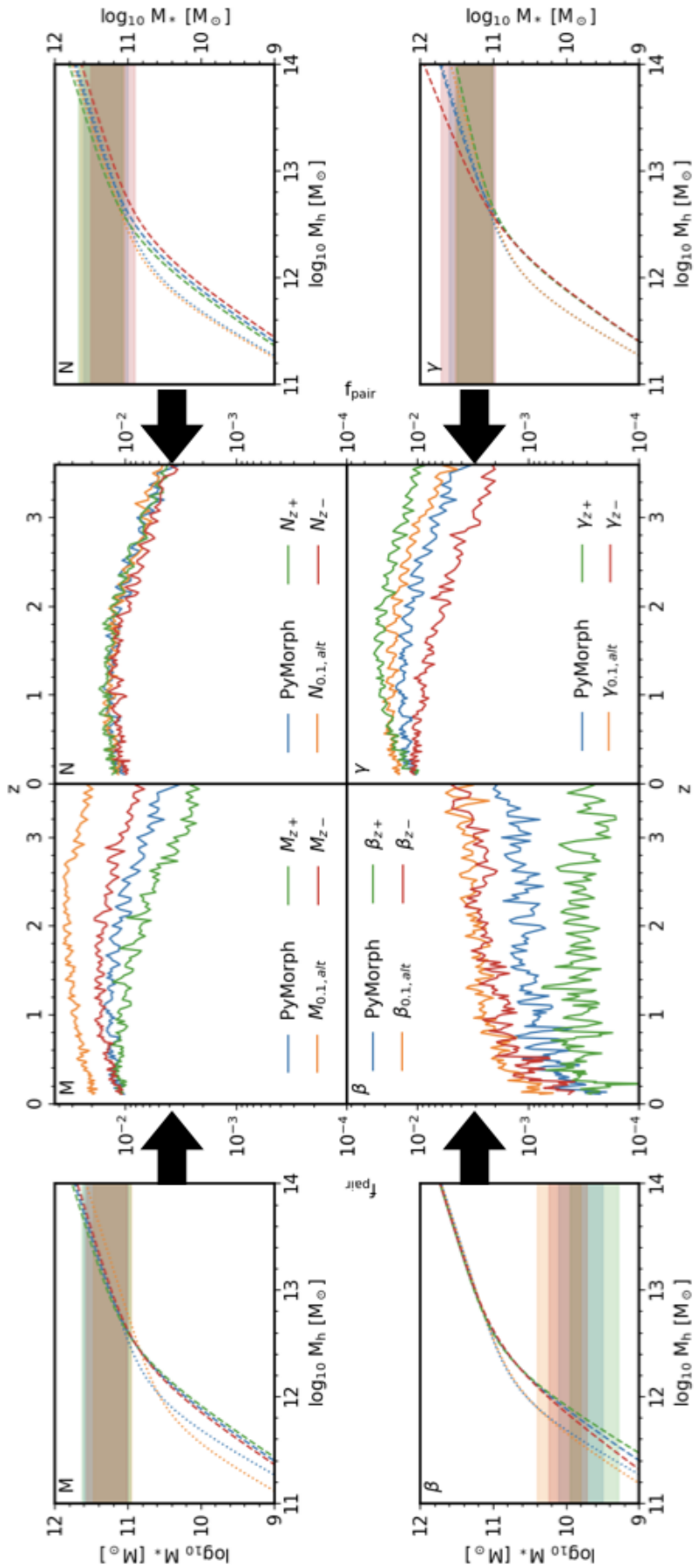

Figure 3. Each of the panel pairs (M, N, β, γ) shows the input stellar-mass-halo-mass relation in the outer plot and the modelled pair fraction evolution in the center plot. Each pair investigates adjustments to the given parameter of the stellar-mass-halo-mass relation (M, N, β, γ). Each pair shows the reference stellar-mass-halo-mass relation 'G18' in blue, the relation adjusted at redshift $z = 0.1$ keeping the same stellar-mass-halo-mass relation evolution parameters in yellow. The red and green lines have the evolution parameter altered such that the evolution parameter is increased or decreased with respect to PyMorph respectively. In the outer (stellar-mass-halo-mass relation) plots dotted lines are $z = 0.1$ relations and dashed lines are $z = 2$ relations the PyMorph relation is shown at both epochs for comparison. Finally the shaded bands in the outer plots show the consistent number density selections used in the center plots.

4.2 Simulation and Observational Results

The observed pair fraction is known to have discrepancies based on the galaxy property used to calculate the ratio. In Man et al. (2016) it is shown that selecting pairs by flux ratio or stellar mass creates differences in the pair fraction evolution. [We theorize in Figures 1 & 2 that different photometries also should create a difference in the pair fraction. In Figure 3 we show a systematic prediction of how photometries should propagate using the stellar-mass-halo-mass relation as a proxy. It is desirable not simply to understand that the pair fraction changes but how it changes in a predictable fashion such that differences can be understood, in this way independent pair fraction studies can be better compared to one another.] In Figures 1 & 2 we show the theoretical effect of the determination of stellar mass on the stellar-mass-halo-mass relation and the propagation of the changes into the pair fraction. Through the use of a toy model in 3 we show systematically how we expect the changes to manifest based on the eight stellar-mass-halo-mass relation parameters. Given this analysis we find that any observation of the pair fraction must be be understood in terms of its implicit observational assumptions. Furthermore, any direct comparison taken between two different pair fraction results should only be undertaken under identical stellar mass derivation assumptions. In this section we show, by making use of STEEL , how small changes to the stellar-mass-halo-mass relation can be used to fit observed pair fractions. We anticipate this modelling could then be used to provide corrections to pair fraction results to allow for fair comparisons.

In Figure 4 we show the pair fraction for galaxies in the mass range $M_* = 10^{10}$ to $10^{10.6}$. The pair fraction is shown for two different stellar-mass-halo-mass relation inputs to STEEL , in blue we show the PyMorph (Sèrsic Exponential) input used as the baseline in Figure 3, in orange the input calibrated to match the Illustris TNG simulation. In the right hand panel we see that the the prediction from STEEL with the TNG calibrated input is in good agreement to the pair fraction extracted directly from the Illustris TNG simulation. The pair fraction predicted using the PyMorph input is 0.5 dex lower, this is to be expected as in the mass range we are considering the Illustris TNG simulation stellar-mass-halo-mass relation is shallower and more pairs are therefore created in a greater mass range of halo mergers.

Figure 5 shows the predicted pair fraction evolution using the two stellar-mass-halo-mass relations from PyMorph and cmodel presented in Section 3.2. The left panel shows each stellar-mass-halo-mass relation at redshift $z = 0.1$ and $z = 2.5$. Following the systematic investigation in Figure 3 we attribute the 0.1 dex difference in pair fraction to the difference in high mass slope between PyMorph and cmodel. The best fit relation from Mundy et al. (2017), shown as black crosses, rises rather than falls as seen from PyMorph and cmodel. Using Figure 3 as a guide growth like this in the pair fraction is best achieved by a stellar-mass-halo-mass relation with a high mass slope that decreases with redshift.

To match the Mundy et al. (2017) pair fractions we use the closest low redshift fit, the cmodel result, and then following Figure 3 where higher γ_z increases the pair fraction at high redshift we alter the parameter from 0.0 to 0.5 in steps of 0.1. In Figure 6 the left panel shows the stellar-mass-halo-mass relation at redshift 0.1 as a black dotted line then coloured lines show the relation at redshift $z = 2$ given the different γ_z parameters. The right panel shows the impact of this evolution on the pair fraction, as predicted higher γ_z increases the pair fraction with redshift and a value of above 0.1 removes the turnover. Comparing to Mundy et al. (2017) we see a value of γ_z between 0.1 and 0.2 best reproduces the rise in pair fraction.

In Paper II we show not all stellar-mass-halo-mass relationship are internally self consistent within a given ΛCDM assembly. Following the average growth of a halo mass bin one can use the stellar-mass-halo-mass relationship to predict the average galaxy growth for this population of haloes, the average satellite accretion should then be less than or at most equal to this both in total accretion and instantaneous rate. In Figure 7 we show the self consistency for four fits. Firstly we show the cmodel fit, then the two γ_z models that are closet to the Mundy et al. (2017) pair fraction, and finally the maximum slope evolution $\gamma_z = 0.5$. For three stellar masses as indicated by the column labels galaxies are chosen at redshift $z = 0.1$ and by following the average halo growth the galaxy is associated to the average galaxy mass and satellite accretion is traced backward in time. The top row shows the total mass predicted by abundance matching (solid lines) and from satellite accretion (dashed lines), the middle row shows the ratio of mass accreted to total mass gained since redshift $z = 3$, the bottom row shows the ratio of instantaneous satellite accretion to instantaneous growth rate. In the middle and bottom rows the solid black lines are at unity and a model that goes above this line is non-physical as more matter would have been accreted than the galaxy growth history can account for. From Paper II we know cmodel to be internally inconsistent, for $\gamma_z = 0.5$ the slow growth at redshift $z = 2$ means satellite accretion is far more rapid than galaxy growth, the $\gamma_z = 0.1$ and 0.2 models are fairly simmilar with the 0.1 model slightly favoured, the total accretion and ratio are good (top and middle rows, green line) the instantaneous rate is slightly high but could be accounted for via a greater loss of mass to the intra cluster medium during a merger[3].

5 DISCUSSION

[We have shown through use of two fits to data and toy models that the observed pair fraction, both in terms of normalization and evolution, is highly sensitive to the photometry used when determining stellar masses. We have explored this effect using the stellar-mass-halo-mass relation to map galaxies into haloes then selecting galaxies at consistent number density so as to be comparing like to like halo substructure as galaxy merger rate is dictated by the mergers of dark matter haloes. We show that the photometry used to create the stellar mass function is of 1st order significance when calculating pair fractions.] The primary goal of this paper is to show the propagation of systematics in galaxy modelling. Specifically we connect the assumptions used to calculate stellar masses from observations to systematics in galaxy pair fractions. In this work we have used two

[3] The models presented here use $f_{loss} = 0.5$ similar to Moster et al. (2018).

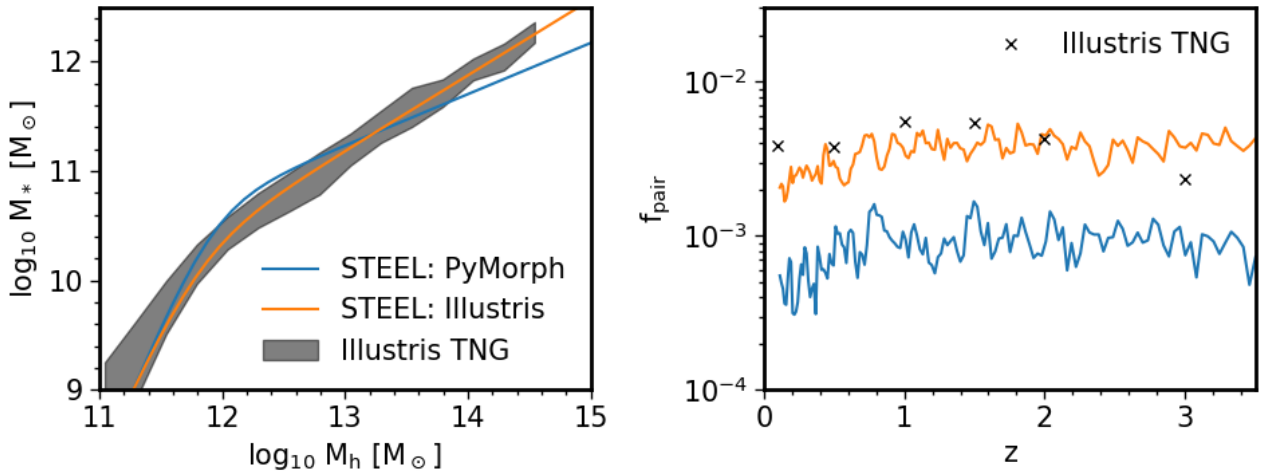

Figure 4. Left: Two stellar-mass-halo-mass relations are shown from STEEL using parameters designed to reproduce the stellar-mass-halo-mass relation found in the Illustrius TNG simulation (Orange line) and the PyMorph(Sèrsic Exponential) fit parameters (Blue line). The shaded region is the output from the Illustris TNG simulation. Right: The pair fraction, for galaxies in the mass range $M_* = 10^{10} M_\odot$ to $10^{10.6} M_\odot$ generated from STEEL is shown for runs using both the stellar-mass-halo-mass relations, lines follow the same colours as the left hand panel. The pair fraction extracted directly from the Illustris TNG simulation is shown using black crosses.

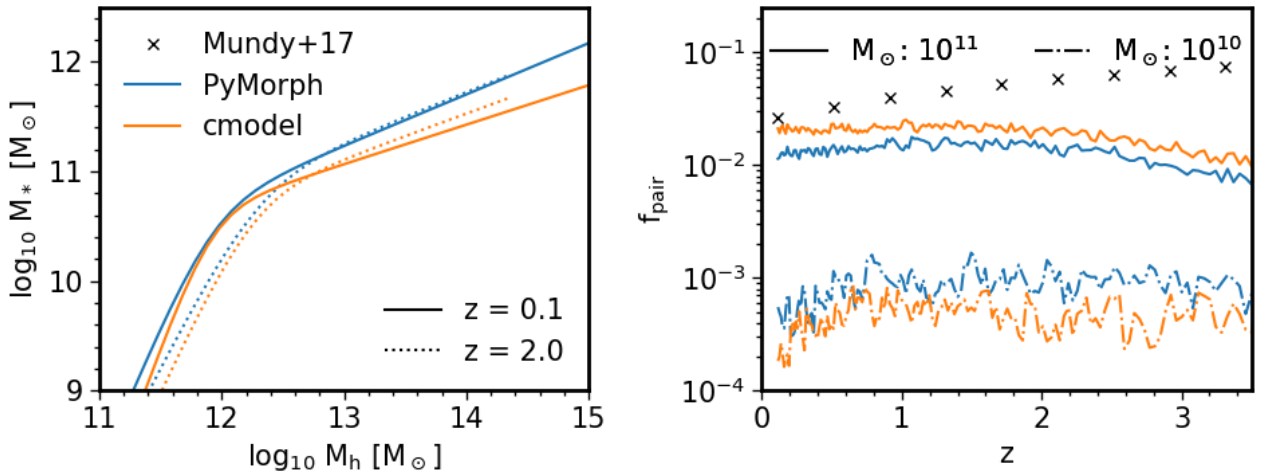

Figure 5. Left: The stellar mass halo mass relations derived from PyMorph (blue) and cmodel (orange) at redshifts 0.1 (solid lines) and 2.0 (dotted lines). Right: The pair fraction evolution for galaxies using both SMHM relations. We make mass cuts, $> 10^{10} M_\odot$ (dashed line) and $> 10^{10} M_\odot$ (solid line), in PyMorph and cmodel. The black crosses show the corresponding best fits for the $> 10^{11} M_\odot$ mass cut from Mundy et al. (2017).

observed stellar mass functions from the SDSS-DR7 observations that use a de Vaucoulers and a Sè rsic + Exponential fit to determine stellar masses, these creating stellar mass functions with different number densities of high mass galaxies. These differences enter our model though the stellar-mass-halo-mass relationship, the the aforementioned stellar mass functions the Sè rsic + Exponential mass function with an enhanced high mass end causes the stellar-mass-halo-mass relationship to have a steeper high mass slope. In addition to the stellar-mass-halo-mass relationships from the observed data we use a relationship extracted to match that of the Illistris simulation, furthermore, we create a toy model where the stellar-mass-halo-mass relationship is directly changed. In each case we find that small changes introduced into the stellar-mass-halo-mass relationship, either directly or from observed data, can have significant effects on the expected pair fractions, as shown in Figures 1,2, & 3. This suggests that tensions in previous observational studies could simply, in large part, be traced back to systematics in stellar mass estimates.

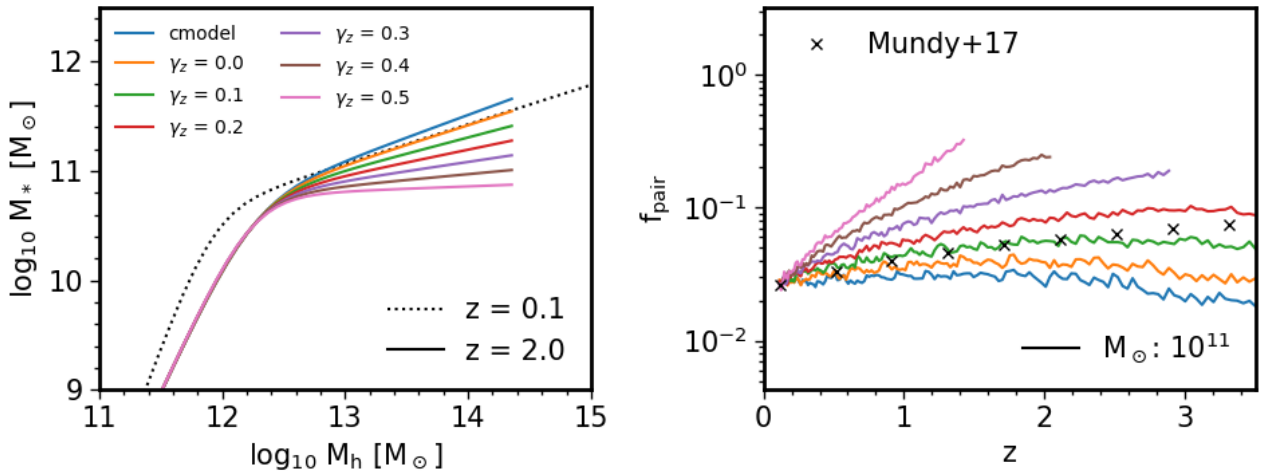

Figure 6. Left: The stellar mass halo mass relations derived from cmodel (black) at redshift $z = 0.1$ (dotted lines) and at $z = 2.0$ (coloured lines) with altered high mass slope evolution parameter. Right: The pair fraction evolution for galaxies each altered stellar-mass-halo-mass relation. The black crosses show the corresponding best fits for the $> 10^{11} M_{\odot}$ mass cut from Mundy et al. (2017).

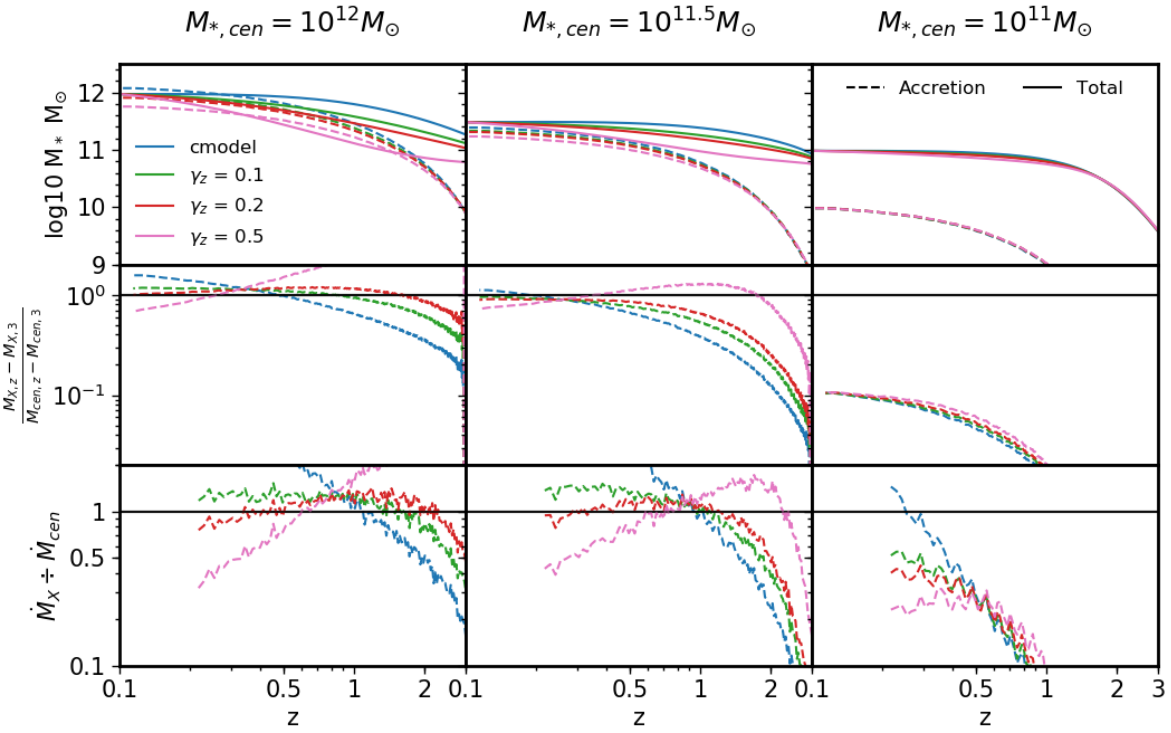

Figure 7. Average 'mass tracks' are shown that have central galaxy masses at redshift $z = 0.1$ of $M_{*,cen} = 10^{12}$, $10^{11.5}$, and 10^{11} $[M_{\odot}]$ from left to right. The satellite galaxy accretion is shown for evolved satellites with a dashed line. The top panels show the total mass of the central (solid lines) and the total mass gained from accretion. The middle panels show the fraction of the total galaxy mass formed from satellite accretion since redshift $z = 3$. The bottom panels show the ratio of the mass accretion rate from satellite galaxies to the mass growth rate of the central galaxy predicted by abundance matching. The black horizontal lines in the second and third rows are at unity. The colours are coded to the high mass slope evolution parameter as shown in the legend.

[Foremost in this work we find that stellar mass selected pair fractions are sensitive to the input stellar mass photometry. The sensitivity found in this work is simmilar to that found in] Man et al. (2016) noticed that the choice between luminosity-selected and stellar-mass selected pairs affected the pair fraction evolution. In this work we have provided a clear framework to properly interpret how input choices create systematic effects in the observed pair fraction and its evolution. Furthermore, it is a common approach to infer the assembly history of galaxies by converting the pair fractions into merger rates by assigning timescales to galaxy pairs (Conselice et al. 2003, 2008; Mundy et al. 2017). [With this approach the difference between an increasing and a decreasing pair fraction implies different formation histories for galaxies some of which may be internally inconsistent as described in Paper II. Here again STEEL can provide greater insight the inputs of STEEL are flexible and can be tuned to match pair fraction observations and check for observational self consistency, furthermore, in STEEL the merging timescales are true to the dark matter assembly therefore the merging history can be considered the true merging history.]

The change from a de Vaucouleurs-based photometry to a Sérsic-Exponential photometry is highlighted as a source of possible future error in pair fraction comparisons in this work, specifically the pair fraction is found to be reduced for the Sérsic-Exponential photometries that predict more massive galaxies and a steeper high mass slope in the stellar-mass-halo-mass relation. It is however reasonable to extend the methodology to a more general case with the techniques presented in this work and in Paper I & Paper II one could reasonably work out the systematic differences created in pair fraction under multiple ΛCDM cosmologies and for any given set of stellar mass functions. We demonstrate a limited example of this capability by showing STEEL can attribute the Illustris pair fraction to a difference in stellar mass function. It is theoretically possible to use a model to derive the expected systematic differences between data sets to be able to add a correction factor to make fair comparisons. A Semi-Empirical model such as STEEL is ideally suited to this data driven analysis as it is flexible and fast to re-tune.

In the era of wide and deep surveys, such as EUCLID, constraining a model using a single data set with consistent photometry becomes a possibility. The advantages of this are twofold, by tuning the stellar-mass-halo-mass relation to a given survey over a large range of redshifts the growth of the stellar mass function over time can be tested against the implied satellite accretion and star formation rate as in Paper II this can be seen as a test of the consistency of the cosmological model or of the consistency of the stellar mass and/or starformation rate estimation, secondly as in Paper I one can test if the high redshift stellar-mass-halo-mass relation produces the low redshift satellite distributions. The constraints on a given photometry, cosmological model, satellite evolution, starformation rate, e.t.c... are still not complete however it will allow nonphysical results to be identified. Furthermore, by making the model widely available and easy to use it can then be used in the manner described above to make systematic adjustments to compare to future data sets.

6 CONCLUSIONS

In this paper we show that the input stellar-mass-halo-mass relation has a significant impact on the pair fraction, in short the steeper the relation the lower the pair fraction. Specifically we compare stellar mass functions created with a de Vaucouleurs-based photometry to a Sérsic-Exponential photometry the latter leading to an enhancement in the number density of high mass galaxies. The resulting effect of these stellar mass functions is a different input stellar-mass-halo-mass relation to steel, the primary difference in in that of the high mass slope with Sérsic-Exponential creating a steeper slope. As expected the Sérsic-Exponential therefore creates a lower pair-fraction. To attempt to explain the difference in pair-fraction evolution with redshift we create a suite of toy models testing different alterations to the stellar-mass-halo-mass relation, it is found that the evolution is linked to the evolution of the high mass slope.

In the context of understanding galaxy assembly and morphological change thorough mergers this work is particularly important. Merger rates are commonly inferred from pair fractions and used to predict rates of mass accretion and the prevalence of major mergers in creating the variations in morphological type. Here a slight change in pair fraction can significantly change the internal consistency of the model by changing the galaxy growth to accretion rate.

The purpose of this paper is not to discredit any work on pair fractions and whilst we favour the PyMorph fit to stellar mass as we have shown the cmodel fits, within errors, can be close to being an internally consistent model. Instead, we show how subtle changes in derivation of stellar mass could lead to large differences in the pair fraction observed, when comparing two different samples it is essential to account for these systematic biases and account for them. Future surveys should look to use fast and flexible modelling alongside data products to be able to properly understand the systematic effects of assumptions made on derived data products.

ACKNOWLEDGEMENTS

We acknowledge extensive use of the Python libraries astropy, matplotlib, numpy, pandas, and scipy. PJG acknowledges support from the STFC for funding this PhD. FS acknowledges partial support from a Leverhume Trust Research Fellowship & from the European Union's Horizon 2020 programme under the AHEAD project (grant agreement #654215).

REFERENCES

Abazajian K. N., et al., 2009, The Astrophysical Journal Supplement Series, 182, 543

Asquith R., et al., 2018, Monthly Notices of the Royal Astronomical Society, 480, 1197

Bernardi M., Meert A., Sheth R. K., Huertas-Company M., Maraston C., Shankar F., Vikram V., 2016, Monthly Notices of the Royal Astronomical Society, 455, 4122

Bernardi M., Meert A., Sheth R. K., Fischer J. L., Huertas-Company M., Maraston C., Shankar F., Vikram V., 2017a, Monthly Notices of the Royal Astronomical Society, 467, 2217

Bernardi M., Fischer J. L., Sheth R. K., Meert A., Huertas-Company M., Shankar F., Vikram V., 2017b, MNRAS, 468, 2569
Conselice C. J., Bershady M. A., Dickinson M., Papovich C., 2003, Astronomical Journal, 126, 1183
Conselice C. J., Rajgor S., Myers R., 2008, Monthly Notices of the Royal Astronomical Society, 386, 909
De Lucia G., Springel V., White S. D. M., Croton D., Kauffmann G., 2006, Monthly Notices of the Royal Astronomical Society, 366, 499
Grylls P. J., Shankar F., Zanisi L., Bernardi M., 2019, MNRAS, 483, 2506
Guo Q., et al., 2011, Monthly Notices of the Royal Astronomical Society, 413, 101
Leja J., van Dokkum P., Franx M., 2013, The Astrophysical Journal, 766, 33
Man A. W. S., Zirm A. W., Toft S., 2016, The Astrophysical Journal, 830, 89
Meert A., Vikram V., Bernardi M., 2015, MNRAS, 446, 3943
Mo H. J., Mao S., White S. D. M., 1998, Monthly Notices of the Royal Astronomical Society, 295, 319
Moster B. P., Somerville R. S., Maulbetsch C., Van Den Bosch F. C., Maccì O A. V., Naab T., Oser L., 2010, The Astrophysical Journal, 710, 903
Moster B. P., Naab T., White S. D. M., 2018, Monthly Notices of the Royal Astronomical Society, 477, 1822
Mundy C. J., Conselice C. J., Duncan K. J., Almaini O., Häußler B., Hartley W. G., 2017, MNRAS, 470, 3507
Negroponte J., White S. D. M., 1983, Monthly Notices of the Royal Astronomical Society, 205, 1009
Nelson D., et al., 2018
Springel V., et al., 2018, Monthly Notices of the Royal Astronomical Society, 475, 676

This paper has been typeset from a TEX/LATEX file prepared by the author.